Investigation of charge trapping parameters in aged XLPE cables at different locations

Ning **LIU** (UK), George **CHEN** (UK), Yang **XU** (China),
nl4g12@soton.ac.uk, gc@soton.ac.uk, xuyang@mail.xjtu.edu.cn

ABSTRACT

The presence of space charge in polymeric high voltage cables will cause electric field enhancement during high voltage application, especially when subjected to high voltage direct current (HVDC) field. In the present paper, cross-linked polyethylene (XLPE) films were peeled from the retired cable section taken from service condition of 2 years by using the microtome. In light of a trapping/detrapping model derived from Poole-Frenkel equations, trapping parameters respectively at three different locations (inner-middle-outer layer) of that cable were estimated through their fitting curves.

INTRODUCTION

Space charge was considered to be both causes and consequences of ageing in polymeric materials [1]. Traps are charge capturing sites inside materials. During high voltage application, particularly for dc condition, space charges will be trapped by those sites hence an amplification of the electric field at certain locations. Resultantly, it will accelerate degradation and even lead to an early failure of insulation materials. Typically, traps at shallow and deep energy levels are respectively related with physical and chemical defects inside materials. In recent years, several models [2-6] were proposed to describe and analyze the trapping-detrapping phenomenon. Initially in [2], a simple trapping-detrapping model was derived from Schottky injection mechanism. Thereafter in [3, 4], a simple trapping-detrapping model was applied to investigate trapping parameters (e.g. trap depth and trap density) of both normal LDPE and gamma-irradiated LDPE samples. Through the comparison of those parameters between those two samples, it was concluded that the trapping parameters estimated from the model, especially that for deep traps, could be used as a diagnostic tool to monitor material ageing. Moreover, another theoretical model developed in [5] was further employed to investigate the trapping parameters of peelings from several XLPE cable sections.

After the removal of voltage, charges detrapping should dominate in the bulk of sample, leading to reduction of charge in the sample. However, the charge released from the traps may be captured again by the other trapping centers. However, those two previous mentioned theoretical models take account of only detrapping process during volts-off tests. In the present paper, a new model was derived from Pool-Frenkel equations, which introduce a retrapping term at depolarization. Samples used in this paper were peeled from a cable section retired from 2-year high voltage alternating current (HVAC) operation condition. PEA technique was performed on those samples to obtain space charge dynamics profiles after the removal of the applied voltage.

THEORETICAL MODEL

Poole-Frenkel effect occurs in the materials of wide band-gap (e.g. insulation materials) where electron/holes can reside in. In our present model, the effect demonstrates the Pool-Frenkel mechanism that the potential barrier height of traps is deducted by columbic force due to positively charged centres. As in equation 1, considering the effect of poling field E, the trap depth E_t could be reduced in the field direction by value ΔV_F, i.e.:

$$E'_t = E_t - \Delta V_F(E) \quad (1)$$

where the maximum reduced height $\Delta V_{Fm}(E)$ of the barrier in the field direction is:

$$\Delta V_{Fm}(E) = -2\left(\frac{e^3 E}{4\pi\varepsilon_0\varepsilon_r}\right)^{\frac{1}{2}} \quad (2)$$

This reduced height happens at when Columbic force between electrons/holes and ionised donors/acceptors (i.e. traps) equals to electrostatic force under the applied field E(further details in [7]). Thus, the rate of thermal excitation of trapped electrons/holes from localized states to the conduction/valence band could be given by:

$$R_{esc} = n\nu_0 \exp(-\frac{E'_t}{kT}) \quad (3)$$

where n is the trapped charge density, T is temperature (300K used in the present paper), k is the Boltzmann constant (~1.38×10^{-23}m^{2}s^{-2}K^{-1}kg), and ν_0 is the attempt to escape frequency (~2×10^{13}Hz at room temperature [7]).

However, our model is applied to the condition when the applied electric field is removed. For the sake of simplicity, we neglect the Pool-Frenkel effect caused by local space charge field, thus E'_t could be approximated as E_t.
Moreover, the rate of capture by trap sites should be proportional to the number density of charges which have been released into the conduction/valence band n_f and the number of unoccupied trap sites density $N - n$, and N is total trap density.

$$R_{cap} = n_f(N - n)\nu_{th}S \quad (4)$$

where ν_{th} is the thermal velocity (= 3.7×10^5m/s for holes in polyethylene material [4]) of electrons or holes and S is capture cross section area of trap sites for charge carriers. Moreover, under assumption that there are no thermal generated free electrons or holes and the only charge carriers in the conduction/valence band are those excited from trap sites, n_f could be written as a subtraction between initial trapped charge density n_0 after the removal of voltage and trapped charges density n, i.e:

$$n_f = n_0 - n \quad (5)$$

Combining equations from (3)-(5), the changing rate total trapped charges can be written as:

$$dn/dt = -R_{esc} + R_{cap}$$
$$= -n\nu_o exp\left\{-\frac{E_t}{kT}\right\} + (N - n)(n_0 - n)\nu_{th}S \quad (6)$$

Solving differential equation in (6) with an initial condition $n(0) = n_0$, the resolution will have the form as shown in equation (7):

$$n(t) = a - b\tanh(ct + d) \quad (7)$$

where a, b, c *and* d are coefficients consisting of unknown trapping parameters N, E_t, S, n_0. To shorten the expressions of parameters a, b, c and d, we make substitutions as in following equations (8.a) and (8.b):

$$A = -Nn_0\left[Sv_{th}\exp\left(\frac{E_t}{kT}\right)\right]^2 \quad (8.a)$$

$$B = \left[v_0 + Sv_{th}\exp\left(\frac{E_t}{kT}\right)(N+n_0)\right]^2 \quad (8.b)$$

Therefore, those four coefficients could be expressed as:

$$a = \frac{0.5v_0\exp\left(-\frac{E_t}{kT}\right)}{v_{th}S} + 0.5(N+n_0) \quad (9.a)$$

$$b = \frac{\exp\left(-\frac{E_t}{kT}\right)\sqrt{A+\frac{B}{4}}}{v_{th}S} \quad (9.b)$$

$$c = \exp\left(-\frac{E_t}{kT}\right)\sqrt{A+\frac{B}{4}} \quad (9.c)$$

$$d = \operatorname{arctanh}\left\{\frac{0.5\left[v_0 - v_{th}S\exp\left(\frac{E_t}{kT}\right)(N-n_0)\right]}{\sqrt{A+\frac{B}{4}}}\right\} \quad (9.d)$$

Through fitted curve using equation (7), the values of a, b, c *and* d could be found. Therefore, trapping parameters could be calculated according to equation (8). In equation (7), all trapping sites in the material are considered to be at the same equivalent energy level E_t with an equivalent cross section area value S. The total trap density equals to N.

If we extend equation (7) to two equivalent levels, i.e. shallow traps and deep traps, equation (7) could be written in a new form:

$$n(t) = a - b\tanh(ct+d) + e - f\tanh(gt+h) \quad (10)$$

where a, b, c *and* d can be used to calculate trapping parameters of shallow traps while e, f, g *and* h could make an estimation for parameters of deep traps.

SAMPLE PREPARATION AND SELECTIONS

Sample Preparation

Samples used in our measurements are peeled from an XLPE cable section which is taken from ac service condition of for 2 years at 110kV. The cable section was peeled from surface to core conductor using a microtome. The cutting edge of the peeling blade must be sharpened to ensure the surface of the peelings is smooth. Otherwise, the PEA measurement results can be affected by scratches on the sample surface. XLPE tape, as shown in figure 3 will come out from the microtome. By adjusting the rotating speed of the microtome and forward moving speed the blade it is possible to obtain XLPE tape with a thickness range of $150\sim200\mu m$. During the peeling, peeled slices were placed into 6 bags in accordance with their different distances to the surface of core conductor and the method of peeling is illustrated in figure 2.

In order to use the outlined method, possible formation of heterocharges needs to be eliminated. Heterocharges can be caused by volatile chemicals ionization in XLPE, during poling times. Therefore, we carried out the degassing treatment by heating up the samples in vacuum oven to 80℃ and maintained there for 48 hours.

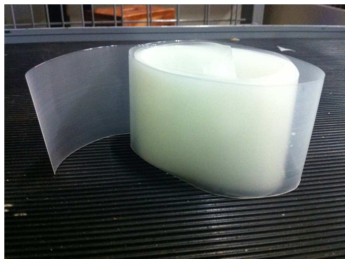

Figure 1: One of XLPE rolls after the cable section was peeled

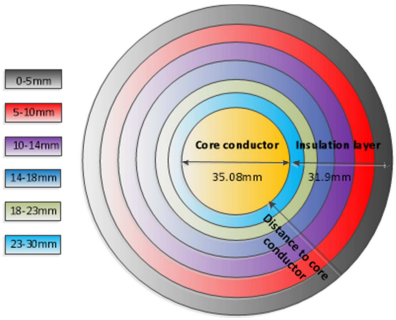

Figure 2: Cable section peeling method according to the different depths in the cable.

Sample Selections

In the present paper, three XLPE strips were taken from the tape rolls selected from: 0~5 mm, 14~18mm, 23~30mm packs, which could be distinguished as the outer, middle and inner region of cable respectively. XLPE slices in proper sizes were cut out of strips. Before degassing treatment on those slices, they were marked to avoid confusions among three layers. The thickness of those selected samples ranges from 140 to 190μm.

EXPERIMENT RESULTS AND ANAYLYSIS

Experimental Methodology

PEA technique was employed to record charge profiles dynamics within 30 minutes after the applied voltage was removed from the sample. Before that, since there are some differences in the thicknesses of XLPE slices, different voltages were applied to make sure the electric fields stressing on the samples remains at 40kV/mm. The stressing times were 6 minutes for every set of measurement. It is assumed that during poling times, 40kV/mm applied on sample for 6 minutes will not alter trapping parameters, e.g. not creating new traps.

Typical Experimental Results on Three Layers of XLPE Samples

Following three figures are selected from many sets of PEA measurements data respectively for three layers. As shown in figures 6~8, for most of depolarization data, bipolar homocharge decay profiles were observed during volts-off test. In line with our previous works on low-density polyethylene (LDPE) in [4], for some of the measurements, injected electrons decay very fast from the cathode. This phenomenon is more common for measurements on samples from the outer and middle layers. As denoted in figures 6 and 7, the negative peak inside bulk which is caused by the injected electrons gradually moves to the left side and eventually becomes an image charge peak on the cathode. It should be noted that in figure 3, the positive image charge peak disappears from the cathode, probably due to the limited resolution of the PEA system. From the viewpoint of trap depth, it shows that samples from the inner layer contain more deep traps, which can capture electrons more easily.

Besides, from figure 4, it can be observed that positive charges in the bulk will drift under the local space charge field to the other side of the bulk and slowly accumulate near the cathode, as indicated by the small arrow in figure 4. This phenomenon was typically observed for the middle-layer sample of the cable, indicating that charges

in the samples have a higher mobility.

FTIR Experimental Results

The Fourrier Transform Infra-Red (FTIR) spectrum are conducted on an IRPrestige-21 spectrometer with wave number vary from 4000cm^{-1} to 400cm^{-1}. The resolution is 4cm^{-1}and 20 scans of signal are averaged. The carbonyl index R is defined as the ratio of the absorption at 1720cm^{-1} (carbonyl band) to the absorption at 2010cm^{-1}, which is not sensitive to oxidation. The carbonyl index characterizes the degree of oxidation for the thermally aged XLPE samples. The value of R could be calculated from equation (11):

$$R = \frac{A_{1720}}{A_{2010}} \tag{11}$$

where A_{1720} is the area of the carbonyl band absorption peak and A_{2010} is the area of 2010 cm^{-1} absorption peak. In this experiment the size of sample is 10×5×0.05 mm. Before the experiment, samples were cleaned by alcohol. To eliminate effects on the test results yielded by alcohol cleaning, samples were placed half an hour under room temperature until dried. The statistical data of 2-year operated cable section is shown in table 1.

Table 1: Carbonyl index of samples

Layers	*Inner layer*	*Middle layer*	*Outer layer*
Carbonyl Index *R*	**0.58**	**0.60**	**0.75**

According to table 1, the degree of oxidation is remarkably most serious in the outer layer. This should be owing to the reason that XLPE at outer section have a better contact with oxygen hence an increase of oxidized sites. However, the degree of ageing should not be simply determined from carbonyl results. Actually, during service condition of extended periods, the samples from the inner insulation layer experience both higher temperature and electric field [9], as in equation (12) suitable for cylindrical insulation cable of one material at ac condition:

$$E(r) = \frac{U}{r ln(\frac{R_0}{R_i})} \tag{12}$$

where U stands for the applied voltage, r is the distance to the center of core conductor, R_0 is external radius of the insulation and R_i is the radius of core conductor. Therefore, it is reasonable to predict that samples from the inner layer have severest degree of ageing. It could be further verified by the estimation of trapping parameters of samples from three layers. Moreover, the results from FTIR experiments should be further correlated with estimated trapping parameters of deep traps.

ESTIMATION OF TRAPPING PARAMETERS

Assumptions

A few assumptions and premises have to be proposed before estimation.

- For calculation of the total trapped charge amount, we only take account of the positive charge peak. Both attenuation and dispersion through the thickness of sample were discarded.
- Traps are uniformly distributed in the sample.
- Sample slices cut from one strip of the same layer were considered to be identical.
- There are no thermally generated electrons/holes in conduction/valence band.

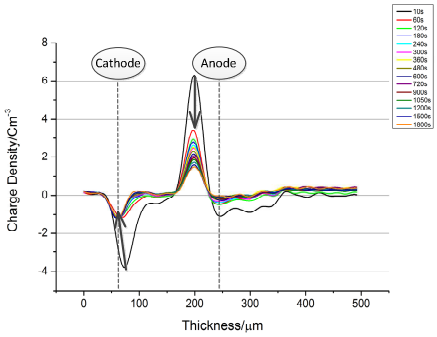

Figure 3: Charge profiles of a 160 μm outer-layer sample after the removal of 6.4kV applied voltage

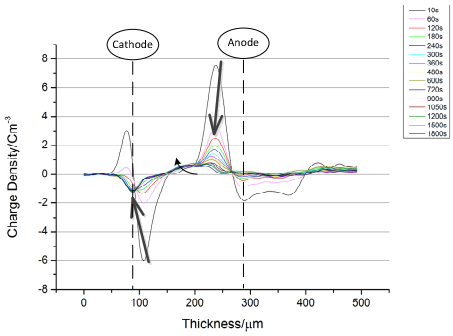

Figure 4: Charge profiles of a 180 μm middle-layer sample after the removal of 7.2kV applied voltage

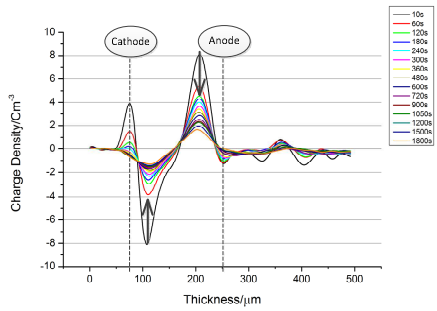

Figure 5: Charge profiles of a 150 μm inner-layer sample after the removal of 6kV applied voltage

Calculation Method

To calculate the total trapped charge Q amount inside bulk, equation (13) applies.

$$Q = \int_0^l |\rho(x,t)| S dx \tag{13}$$

where l is the thickness of positive charge layer, S is the electrode area, t is depolarization time, and x is the coordinate on horizontal axis. Therefore, the density of the trapped charges n is:

$$n = \frac{Q}{l \cdot S \cdot q} \tag{14}$$

PEA measurement is rather sensitive to environmental factors: temperature, moisture, mechanical stresses and silicone oil. Therefore, even we applied the same electric field with an identical stressing time, measurement results may more or less differ from each other. To minimize the

occasional errors caused by those uncontrollable factors, we selected some similar results from measurements of each layer and average trapped charge densities at each depolarization time, as shown in figures 6 to 8.

Fitting Curves and Estimation on Trapping Parameters

Either equation (7) or (10) can be utilized to be the curve fitting equation by MATLAB curve fitting tool.

If equation (7) applies, curve fitting could be found as in figure 9. However, due to limitation of single-level detrapping model, R-square[1] values of curve fitting using equation (7) for those three sets of scattering points are just around 0.9, and details can be found in table 2.

Meanwhile, coefficients a, b, c, d for three insulation layers could be obtained by fitting curves, as in table 3.

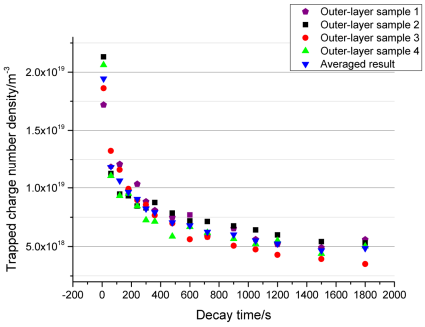

Figure 6: Scattering data points of 4 outer layer samples and their averaged result.

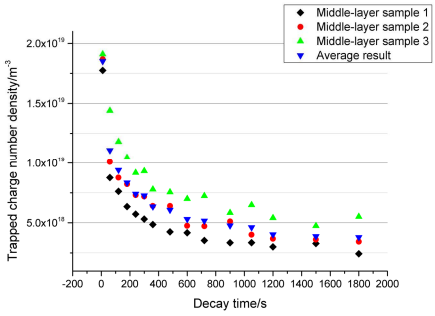

Figure 7: Scattering data points of 3 middle layer samples and their averaged result.

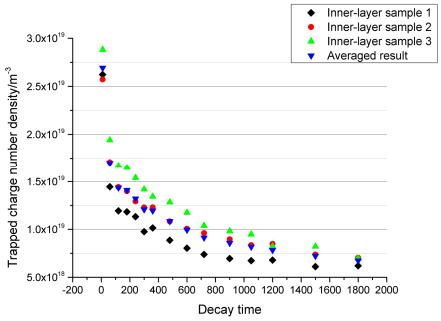

Figure 8: Scattering data points of 3 inner layer samples and their averaged result.

1: R-square is the square of the correlation between the response values and the predicted response values. With a value closer to 1, it indicates that a greater proportion of variance is accounted for by the model.

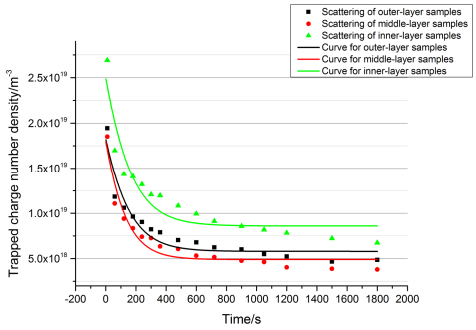

Figure 9: Curve fitting results using equation (7).

Table 2: R-square values by using equation (7)

Layers	*Outer layer*	*Middle layer*	*Inner layer*
R-square values	**0.9131**	**0.9314**	**0.8971**

Table 3: Values for coefficients a, b, c, d

Coefficients	*Outer layer*	*Middle layer*	*Inner layer*
a	3.8900×10^{19}	4.3600×10^{19}	5.1100×10^{19}
b	3.1100×10^{19}	3.8700×10^{19}	4.2500×10^{19}
c	0.003717	0.004354	0.003493
d	0.7319	0.7951	0.7174

By solving the equations from (9a)-(9d), trapping parameters estimated using single-level detrapping model could be found, as in table 4.

Table 4: Trapping parameters for single equivalent level trap

Trapping parameters	Outer layer	Middle layer	Inner layer
N/m^{-3}	2.2897×10^{19}	2.2394×10^{19}	3.2263×10^{19}
n_0/m^{-3}	1.8238×10^{19}	1.8008×10^{19}	2.4950×10^{19}
E_t/eV	0.9346	0.9282	0.9374
S/m^2	3.0350×10^{-28}	3.0407×10^{-28}	2.2213×10^{-28}

If equation (10) applies, much better curve fitting results with higher R-square values above 0.99 could be obtained, as show in table 5.

Table 5: R-square values by using equation (7)

Layers	Outer layer	Middle layer	Inner layer
R-square values	0.9959	0.9953	0.9963

And the fitting curves obtained by using the two-level detrapping model, i.e. equation (10), are shown in figure 10. Thus from the three fitting results, coefficients a, b, c, d, e, f, g and h were obtained in table 6.

Thereafter, solving equation from (9a) to (9d) twice according to coefficients in table 6, trapping parameters respectively for shallow and deep traps could be found in table 7.

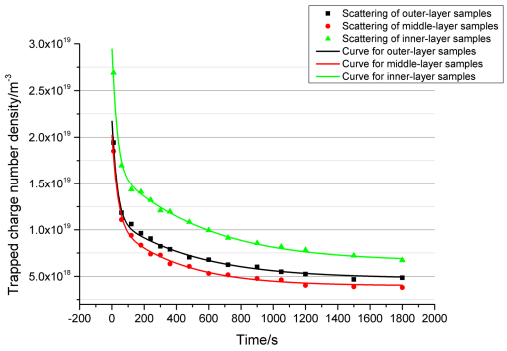

Figure 10: Curve fitting results using equation (10).

Table 6: Values of coefficients a, b, c, d, e, f, g, h

Coefficients	*Outer layer*	*Middle layer*	*Inner layer*
a	3.3000x10^{19}	3.7200x10^{19}	4.21000x10^{19}
b	2.9800x10^{19}	3.5200x10^{19}	3.8600x10^{19}
c	0.01738	0.01501	0.01775
d	0.7500	0.9000	0.7850
e	2.1500x10^{19}	2.1300x10^{19}	3.5100x10^{19}
f	1.9900x10^{19}	1.9300x10^{19}	3.2000x10^{19}
g	0.001110	0.001385	0.001006
h	0.8300	0.8000	0.8472

Table 7: Trapping parameters for shallow and deep traps

Trapping parameters	*Outer layer*	
	Shallow traps	Deep traps
N/m^{-3}	1.4280x10^{19}	8.3231x10^{18}
n_0/m^{-3}	1.4073x10^{19}	7.9585x10^{19}
E_t/eV	0.8913	0.9609
S/m^2	1.5763x10^{-27}	1.5075x10^{-28}
Trapping parameters	**Middle layer**	
	Shallow traps	**Deep traps**
N/m^{-3}	1.2080x10^{19}	9.5709x10^{18}
n_0/m^{-3}	1.1986x10^{19}	8.4841x10^{19}
E_t/eV	0.8919	0.9566
S/m^2	1.1525x10^{-27}	1.9395x10^{-28}
Trapping parameters	**Inner layer**	
	Shallow traps	**Deep traps**
N/m^{-3}	1.6817x10^{19}	1.5961x10^{19}
n_0/m^{-3}	1.6795x10^{19}	1.3033x10^{19}
E_t/eV	0.8898	0.9645
S/m^2	1.2428x10^{-27}	8.4966x10^{-29}

DISCUSSION

In line with our previous work on normal and gamma-irradiated LDPE samples [4], it is reasonable to conclude that trapping parameters, especially for deep traps, can be used a diagnostic tool of ageing. From trapping parameters estimated from equation (7), referring to figure 11, trap density of the inner-layer samples is much larger than that from the other two layers. Meanwhile, overall equivalent trap depth of the inner-layer samples is deeper than that of the other two layers whereas the trap depth of samples from the inner and outer layers is quite close to each other. Moreover, comparing the trapping parameters of samples from the middle and outer layers as in table 4, trap density only experiences a slight variation but the trap depth of the outer layer is obviously deeper than that of the middle layer. Therefore, charges could more easily release from traps in the middle-layer samples because of their relatively shallower overall equivalent trap depth. This could explain the charges movement phenomenon during the test on the middle-layer sample, as in figure 4.

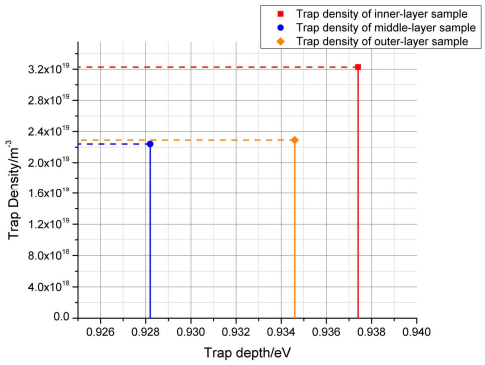

Figure 11: Comparisons on single-level trap depths and their densities for samples at different locations.

Regarding to trapping parameters estimated from equation (10), as shown in table 7, it should be noted that shallow traps were initially almost fulfilled with charges. This indicates that charges prefer to fill shallower energy levels rather than deep ones. Clearly from figure 12, samples from the inner insulation layer have a larger amount of traps, especially for deep traps. This is probably caused by operation condition at the inner layer. From figure 2, the distances to core conductor center r are 19.54~26.54mm, 31.54-35.54mm, 44.54~49.54mm, respectively for sample from the inner (23-30mm), the middle (14~18mm) and the outer (0~5mm) layers. According to equation (12), the samples at 23-30mm depth should have experienced an electric field 1.87~2.54 times larger than that at the outer surface of the insulation (r =49.54mm), while the value ranges are 1.39~1.57 for the middle layer samples and 1~1.11 for the outer layer samples. Moreover, according to what have been measured and modelled in [10], the temperature in a XLPE cable is higher in the region close to the conductor. Therefore, the significant increase of trap density and trap depth at the inner layer could be attributed to the most severe service conditions. Nevertheless the deep trap density of the middle and the outer layer are quite close, and that from the middle layer is little larger. In term of deep trap depth, the outer layer is deeper than that of the middle layer. This result might be due to that the degree of oxidation is most serious at the outer layer, referring FTIR measurement result in table 1. Oxidative sites correlate with introducing chemical defects into the materials and thus might deepen the trap depth and create more deep traps [8].

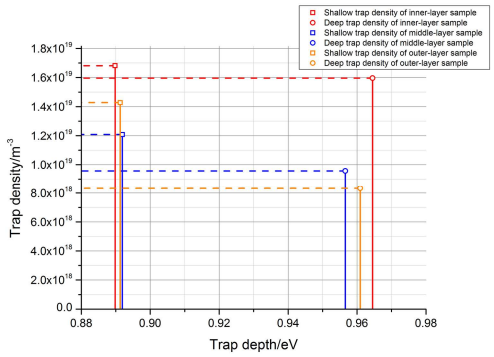

Figure 12: Comparisons on shallow and deep trap depths and their densities for samples at different layers.

Cross section areas S were also calculated as in tables 4 and 7. No direct relations were found between this parameter and the degree of ageing. Despite that, if we plot the trap depth versus cross section area (in tables 4 and 7), it could be noted that the cross section area values are generally smaller when the trap depth get deeper except for first two datapoints. As shown from left to right in figure 13, values of the cross section area could be distinguished as three groups, which are respectively from shallow traps, single-level traps, and deep traps. Therefore, according to the definition of S, figure 13 might indicate that for traps at deeper depth it is harder to capture charge carriers.

Although, the cable peelings used for measurements were taken from ac conditions, the approach to analyse the degree of ageing in present paper is also suitable for HVDC cables. Moreover, for cables in service condition of HVDC, temperature distribution should be similar with that under ac condition but the electric field distribution could be more complex [9].

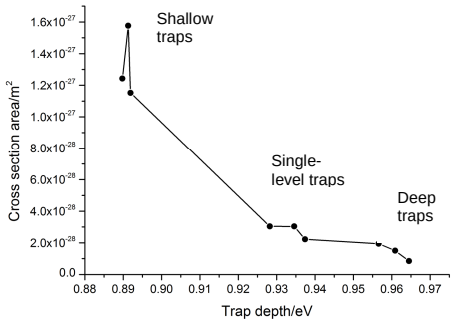

Figure 13: Scattering plot of E_t-S

CONCLUSIONS

Through the experimental and numerical simulation works in present paper, several important conclusions can be drawn as below::

- From FTIR measurement results, the degree of oxidation among three layers could be found by the carbonyl index values. The oxidation degree of aged cable at the outer layer is remarkably higher than that at the other two layers.
- By using the trapping parameters estimated from equation (7), samples from the middle layer have a shallowest trap depth. This might give rise to the highest mobility at the middle layer, which can be proved by charge drifting phenomenon during volts-off test on such sample.
- Through trapping parameters obtained from the equation (10), samples from the inner insulation are severest aged than that at the other two layers. However, through comparisons between those trapping parameters between middle and outer layers, it is hard to evaluate the degree of ageing between those two layers. It could be owing to more chemical defects brought by oxidation at the outer layer.

REFERENCES

[1] G. Mazzanti, G. Montanari, and L.A. Dissado, 2005, "Electrical aging and life models: the role of space charge," IEEE Transactions on Dielectrics and Electrical Insulation, vol. 12, no. 5, 876–890.

[2] G. Chen and Z. Xu, 2009, "Charge trapping and detrapping in polymeric materials," Journal of Applied Physics, vol. 106, no. 12, 123707.

[3] T. Zhou, G. Chen, R. Liao, and Z. Xu, 2011. "Charge trapping and detrapping in polymeric materials: Trapping parameters," Journal of Applied Physics, vol. 110, no. 4, 043724.

[4] N. Liu, and G. Chen, 2013, "Modeling of charge trapping/detrapping characteristics in polymer materials and its relation with ageing", Electrical Insulation and Dielectric Phenomena, Annual Report., Conference on, accepted in publishing.

[5] A. Tzimas, S. M. Rowland and L.A. Dissado, 2012, "Effect of electrical and thermal stressing on charge traps in XLPE cable insulation", IEEE Transactions on Dielectrics and Electrical Insulation, vol. 19, no. 6, 2145-2154.

[6] L.A. Dissado, V. Griseri, W. Peasgood, E.S. Cooper, K. Fukunaga, and J. C. Fothergill, 2006, "Decay of space charge in a glassy epoxy resin following voltage removal", IEEE Transactions on Dielectrics and Electrical Insulation, vol. 13, no. 4, 903-916.

[7] L.A. Dissado and J.C. Fothergill, 1992, "Electrical degradation and breakdown in polymers", 9th ed., P. N. Morgan, D.V. and K. Overshott, Eds. Peters Peregrinus Ltd., London, United Kingdom.

[8] D. Marsacq, P. Hourquebie, L. Olmedo, and H. Janah, 1995, "Effects of physical and chemical defects of polyethylene on space charge behaviour," Electrical Insulation and Dielectric Phenomena, Annual Report., Conference on, Virginia Beach, USA, 672-675.

[9] M.J.P. Jeroense and P.H.F. Morshuis, 1998, "Electric Fields in HVDC Paper-Insulated Cables", IEEE Transactions on Dielectrics and Electrical Insulation, vol. 5, no. 2, 225-236.

[10] T.S. Adel-Salam, R. Hackam and A.Y. Chikhani, 1990, "Temperature distribution in the dielectric insulation of distribution cables", Electrical Insulation and Dielectric Phenomena, Annual Report., Conference on, Pocono Manor, PA, 514 – 519.